Nuclear Fusion Driven by Coulomb Explosion of Methane Clusters†

Isidore Last and Joshua Jortner*

School of Chemistry, Tel-Aviv University, Ramat Aviv, Tel Aviv 69978, Israel

Received: March 4, 2002

Multielectron ionization and Coulomb explosion of methane clusters $(CA_4)_n$, A = H, D, and T, in very intense ($I = 10^{18}-10^{19}$ W cm^{-2}) laser fields were studied using classical dynamics simulations. The products of Coulomb explosion involve light A^+ ions (p, d, and t nuclei) with energies up to 20 keV, C^{4+} ions at $I = 10^{18}$ W cm^{-2}, and C^{6+} ions (carbon nuclei) with energies up to 110 keV at $I = 10^{19}$ W cm^{-2}. Important advantages of nuclear fusion driven by Coulomb explosion of methane $(C^{4+}A_4^+)_n$ and $(C^{6+}A_4^+)_n$ heteronuclear clusters pertain to energetic effects, with the heavy multielectron ions driving the light H^+, D^+, or T^+ ions (d or t nuclei) to considerably higher energies than for homonuclear deuterium clusters of the same size, and to kinematic effects, which result in a sharp high-energy maximum in the light-ion spectrum for the $(C^{4+}A_4^+)_n$ and$(C^6\ A_4^+)_n$ clusters. We studied the energetics of Coulomb explosion in conjunction with isotope effects on the product A^+ and C^{k+} ions energies and established the cluster size dependence of dd and dt fusion reaction yields from an assembly of Coulomb-exploding clusters. The C^{6+} nuclei produced by Coulomb explosion of $(C^{6+}D_4^+)_n$ ($n = 5425$) clusters are characterized by an average energy of $E_{av} = 65.2$ keV and a maximum energy of $E_M = 112$ keV. A search was undertaken for the $^{12}C^{6+} + {}^1H^+$ fusion reaction of astrophysical interest.

I. Introduction

The search for nuclear fusion driven by cluster dynamics stems from the 1989 Brookhaven experiments[1,2] on high-energy deuterated cluster−wall collisions, which, unfortunately, did not provide information on cluster impact fusion. Compelling experimental and theoretical evidence for nuclear fusion reactions driven by Coulomb explosion (NFDCE) of an assembly of deuterium-containing molecular clusters was recently advanced.[3−6] The irradiation of molecular clusters by ultrashort (tens of femtoseconds) and ultraintense ($I = 10^{15}-10^{19}$ W cm^{-2}) laser pulses results in Coulomb explosion of these clusters and in the formation of high-energy atomic ions.[7−18] Zweiback et al.[3,4] demonstrated that the Coulomb explosion of large deuterium clusters (cluster radii $R \approx 10-50$ Å) provides deuterons that are capable of performing the dd fusion reactions[19]

$$d + d \rightarrow He^3 + n + 3.27\ MeV \quad (1a)$$

$$d + d \rightarrow t + p + 4.03\ MeV \quad (1b)$$

The perspectives of the fusion reaction 1a for the production of time-resolved (100 ps−10 ns) neutron pulses are of considerable interest.[4] When the clusters contain a mixture of deuterium and tritium atoms, the NFDCE can also result in the dt fusion reaction[19]

$$d + t \rightarrow He^4 + n + 17.6\ MeV \quad (2)$$

We proposed and demonstrated[5,6] that an effective way to produce energetic deuterons and tritons for the NFDCE is provided by Coulomb explosion of molecular heteronuclear clusters $(A_lB_k)_n$, where the light one-electron A atoms (A = D or T) are bound to heavy multielectron B atoms. Our simulations of the NFDCE of heteronuclear water clusters $(D_2O)_n$ and $(T_2O)_n$ [5,6] demonstrated that the highly charged O^{6+} ions provide a trigger for driving the light D^+ and T^+ ions to a considerably higher kinetic energy than is obtained in homonuclear D_n and T_n clusters of the same size. For example, the maximum kinetic energy, E_M, of deuterons produced by Coulomb explosion of a homonuclear D_{3367} cluster with radius $R_0 = 25.4$ Å is $E_M = 1.9$ keV, whereas the heteronuclear cluster $(D_2O)_{2172}$ with almost the same radius $R_0 = 25$ Å provides deuterons with $E_M = 10.8$ keV.[6] On the experimental front, Coulomb explosion of molecular heteronuclear clusters with deuterium was experimentally studied for ammonia clusters $(ND_3)_n$.[7] Coulomb explosion of heteronuclear clusters with hydrogen atoms was studied, in particular for methyl iodine clusters[13] and hydrocarbons.[15] However, the possibility of nuclear reactions was not considered for these interesting systems. A heteronuclear system providing deuterons for nuclear fusion from an aerogel with absorbed deuterium was recently suggested.[20]

In this paper, we consider the NFDCE of heteronuclear methane $(CA_4)_n$, A = H, D, and T, clusters. The methane clusters, in analogy with the water clusters previously studied by us,[5,6] are expected to provide energetic nuclei of the light A atoms that are driven to high energies by the multicharged C^{k+} ions. Also the multicharged C^{k+} ions become highly energetic particles. In the case of full ionization ($k = 6$), the carbon nuclei can contribute to nuclear reactions. Despite intrinsic interest in the reactions of C^{6+} nuclei for astrophysical applications,[21,22] the cross sections of such reactions are very low.[23] We present a calculation of the reaction yields for the d + d and d + t NFDCE of methane clusters. The energy spectrum of the reagent nuclei is determined here, as in our previous studies,[5,6] by the simulation of the ionization and Coulomb explosion processes in these clusters. We hope that these calculations will be subjected to experimental scrutiny.

† Part of the special issue "R. Stephen Berry Festschrift".
* To whom correspondence should be addressed.

10.1021/jp0206121 CCC: $22.00 © 2002 American Chemical Society
Published on Web 09/20/2002

II. Methodology of the Simulations

In the present work, the simulations of cluster multielectron ionization and Coulomb explosion were performed for a Gaussian-shaped laser pulse with a temporal half-full width at a half-maximum of 25 fs. The field frequency is $\nu = 0.35$ fs^{-1}, corresponding to a photon energy of 1.44 eV. Taking into account that the radii of the clusters considered by us are considerably smaller than the penetration depth of the laser radiation,[24] we assume that the light intensity is independent of the spatial coordinates.

Prior to the switching on of the laser field, the cluster is initially composed of neutral molecules. After the laser field is switched on, the process of cluster inner ionization starts, resulting in the removal of bound electrons from their host atoms and the transformation of neutral atoms into charged ions. The unbound electrons generated by the inner ionization form a plasma within the cluster that is initially neutral. The laser field can remove these electrons from the cluster to infinity, resulting in the subsequent process of outer ionization. Concurrently, outer ionization is accompanied and followed by Coulomb explosion. In the dynamic simulation of cluster ionization, the bound electrons are not explicitly treated, and the inner ionization is described as the generation of unbound electrons.[25−27] The methodology of the present simulations of cluster ionization and Coulomb explosion is identical to our previous studies.[5,6,28] It is based on the sudden inner cluster ionization (SICI) approximation. The SICI approximation implies that, at the starting point for the outer cluster ionization and at the temporal onset of Coulomb explosion ($t = 0$), all of the relevant electrons are already removed from their host atoms and become unbound electrons. It is also assumed that, at $t = 0$, the unbound electrons are motionless and located in the proximity of their host atoms. Such an approach significantly simplifies the simulation by excluding from it the initial stage of the inner ionization process.[28] Detailed numerical studies[6,26] have established that the time scale of the inner ionization of large Xe_n, $(D_2)_n$, and $(D_2O)_n$ clusters ($n = 50-4000$) in a laser field of $I = 10^{16}-10^{18}$ W cm^{-2} (and frequency of 0.35 fs^{-1}) is in the range of 1−2 fs. This time scale is sufficiently short to warrant the validity of the SICI approximation. The unbound electrons and the ions are considered as classical particles.[25,26,28] The unbound electrons can be treated classically when their de Broglie wavelength λ is considerably smaller than the internuclear spacing d. According to our previous simulations,[6] the average kinetic energy of the electrons increases strongly with the laser intensity I and represents $E_e > 150$ eV at a laser intensity of $I = 5 \times 10^{15}$ W cm^{-2}. Such an energy corresponds to the wavelength $\lambda \approx 1$ Å, which is much smaller than the C−C distance $d = 4.4$ Å in methane clusters. Accordingly, we expect that, for $I > 5 \times 10^{15}$ W cm^{-2}, the quantum effects of the electron motion are not of considerable importance, so that the classical approach can be accepted. The classical simulations of the molecular dynamics of the unbound electrons are performed on the femtosecond time scale ($10^{-15}-10^{-13}$ s), using attosecond (10^{-18} s) time steps.

In the present work, outer ionization and Coulomb explosion simulations were performed for methane clusters $(CA_4)_n$, with an emphasis on the deuterium containing, A = D, clusters. The clusters are subjected to laser irradiation in the intensity range $I = 10^{18}-10^{19}$ W cm^{-2}. The clusters are described as being made up of uniformly distributed CD_4 molecules with a C−D distance of 1.09 Å. The density of the $(CD_4)_n$ clusters is taken to be equal to the density of liquid methane,[29] e.g., $\rho = 0.016$ Å^{-3} per molecule. The results are not expected to be sensitive to the simplifications used here for the structure of the clusters. We treat the $(CD_4)_n$ clusters with the number of molecules $n =$ 201, 459, 1061, 2171, 3463, and 5425 and the corresponding radii $R_0 = 14.1$, 18.9, 25.2, 31.8, 37.0, and 42.9 Å. The products of Coulomb explosion of these clusters are D^+ ions (deuterons) and carbon ions C^{k+}. To study the isotope effects on Coulomb explosion, simulations of hydrogen-$(CH_4)_n$ and tritium-containing $(CT_4)_n$ clusters were also performed for $n = 2171$ clusters.

Within the framework of the SICI approximation, one needs to determine the level of carbon atom ionization. In molecular clusters, the barrier suppression mechanism[30] for atomic multielectron ionization dominates over the collisional ionization mechanism, so that the ionization level of the C^{k+} ions depends on the ionization field strength F_{ion}[26,30]

$$|eF_{ion}| > I_k^2/4B(k+1) \tag{3}$$

where $B = 14.385$ eV/Å and I_k is the ionization potential (in electronvolts) of the k-fold charged ion. According to eq 3, the field strength is $eF_{ion} > 3.2$ eV/Å for the light A (H, D, T) atoms ($I_0 = 13.6$ eV), and $eF_{ion} > 2.2$, 5.2, 13.3, 18, 535, 690 eV/Å for $k = 0-5$ for the C atom ($I_k = 11.3$, 24.4, 47.9, 64.5, 392, and 488 eV for $k = 0-5$, respectively[31]). At the pulse peak for $I = 10^{18}-10^{19}$ W cm^{-2} considered herein, the field strength amplitudes ($eF_0 = 2.745 \times 10^{-7} I^{1/2}$ eV/Å, with I in W cm^{-2}) are in the range $eF_0 = 274-868$ eV/Å. The ionization processes in our simulations start when the laser intensity I is four times lower than at the pulse peak. Consequently, at the beginning of the ionization processes ($t = 0$), the field strength range is $eF_0 = 137-434$ eV/Å. Such a field strength is sufficiently strong to ionize the light A (H, D, T) atoms and to remove the valence electrons from the C atom. The removal of the first 1s electron from C^{4+} occurs at field strengths of $eF_{ion} > 535$ eV/Å, which are considerable larger than the field strength of the laser intensity of $I = 10^{18}$ W cm^{-2} ($eF_0 = 274$ eV/Å). Accordingly, at $I = 10^{18}$ W cm^{-2}, the inner electrons are intact, whereas all valence electrons are removed so that the carbon atoms become C^{4+} ions. The C^{4+} ions provide a trigger for driving the light D^+ ions (deuterons d) to high kinetic energies. At even higher laser intensities, corresponding to field strengths of $eF_{ion} > 690$ eV/Å, C atoms are deprived of all of their inner electrons and become carbon nuclei C^{6+}. This criterion is fulfilled at the peak field strength ($eF_0 = 868$ eV/Å) of the laser intensity $I = 10^{19}$ W cm^{-2}. However, at the beginning of the pulse ($t = 0$), when the field strength is 434 eV/Å, which is about one-half of the pulse peak, the laser field can remove only the first 1s electron but not the second one. Taking into account the Gaussian shape of the pulse, we found that the laser field exceeds the minimum of 535 eV/Å required to remove the second 1s electron at $t = 5$ fs, which is a short time compared to the pulse width of 25 fs. This time might become even shorter as a result of the ignition mechanism, which enhances the inner ionization.[32] From these considerations we infer that, in the framework of the SICI approximation, a methane cluster can be considered at $I = 10^{18}$ W cm^{-2} as a $(C^{4+}D_4^+)_n$ ionic frame, which initially yields $N_e = 8n$ unbound electrons. Considering the pulse intensity of $I = 10^{19}$ W cm^{-2}, we ignore the short delay (of ∼5 fs) in the ionization of the last carbon electron and consider a cluster as a $(C^{6+}D_4^+)_n$ ionic frame with $N_e = 10n$ initially unbound electrons.

III. Isotope Effects

The description of the Coulomb explosion of clusters is simplified in the case of vertical ionization, which involves a

separation of the time scales between the removal of all unbound electrons from the cluster (outer ionization) and the cluster spatial expansion. This picture provides a semiquantitative description of the energetics and the time scales for Coulomb explosion.[33] For a homonuclear cluster with an identical charge q on each atom and a uniform atomic density ρ, the final kinetic energy of an ion is equal to its initial potential energy in the charged cluster[6]

$$E(R) = \left(\frac{4\pi}{3}\right)Bq^2\rho R^2, \quad R \le R_0 \tag{4}$$

where R is the initial distance of the ion from the cluster center and R_0 is the neutral cluster radius. The kinetic energy E_M has a maximum value for ions initially located at the cluster surface at $R = R_0$, which is given by[3,5,6]

$$E_M = \left(\frac{4\pi}{3}\right)Bq^2\rho {R_0}^2 \tag{5}$$

The energy distribution $P(E)$ inferred from eq 4 is[6]

$$P(E) = \frac{3}{2}(E/{E_M}^3)^{1/2}, \quad E \le E_M \tag{6}$$

and

$$P(E) = 0, \quad E > E_M \tag{6'}$$

The energy distribution in eqs 6 and 6′ provides the average energy

$$E_{av} = \left(\frac{3}{5}\right)E_M = \left(\frac{4\pi}{5}\right)Bq^2\rho {R_0}^2 \tag{7}$$

Using the relation for the number n of atomic constituents, $n = (4\pi/3)\rho {R_0}^3$, we obtain $E_{av} \propto n^{2/3}$. The dependence of E_{av} on the number of particles is

$$E_{av} = \left(\frac{36\pi}{125}\right)^{1/3}Bq^2\rho^{1/3}n^{2/3} \tag{8}$$

This result is in accord with the expression for the Coulomb energy within the liquid drop model of nuclear and cluster matter.[34]

The E_M and E_{av} energies for homonuclear clusters are proportional to ${R_0}^2$ (or $n^{2/3}$), do not depend on the laser intensity I, and exhibit a minor isotope effect due to the cluster density ρ. According to the simulations performed for D_n and T_n clusters, the simple dependence of E_M on ρ, q^2, and ${R_0}^2$ expressed by eq 5 is well satisfied in the limit of the vertical ionization conditions.[5,6] The energy of ions increases with their charge as q^2, so that multielectron atoms (e.g., Xe atoms) with $q \gg 1$ can provide very high energies of about 1 MeV.[8,11] Deviations from eqs 5 and 7 are manifested with E_M and E_{av} becoming smaller than predicted from these relations when the laser intensity I decreases below some "critical" value $I_{cr}(R_0)$,[5] which is insufficient to induce the effective vertical ionization, e.g., $I < 2 \times 10^{16}$ W cm^{-2} for D_{8007} ($R_0 = 34$ Å).[6] A small positive deviation from the relation $E_M \propto {R_0}^2$ (eq 5) was also detected at very strong laser intensities $I > 10^{18}$ W cm^{-2} because of the direct acceleration of ions by the outer field.[6]

In the case of heteronuclear clusters, the final kinetic energies of the ions are determined both by energetic effects and by kinematic effects. Consider first the energetic effect. If one assumes that the velocity of all ions located at distance R from the cluster center is the same, regardless of their mass and charge, then we obtain, in analogy with the homonuclear cluster (eqs 5 and 7), the energetic contributions to the maximum and the average energies[6]

$$E_M = \left(\frac{4\pi}{3}\right)B(lq_A + kq_B)q\rho {R_0}^2 \tag{9}$$

$$E_{av} = \left(\frac{4\pi}{5}\right)B(lq_A + kq_B)q\rho {R_0}^2 \tag{10}$$

with ρ being the molecular density and q being equal to q_A or q_B for light and heavy ions, respectively; in the case of methane clusters, $k = 1$, $l = 4$, $q_A = 1$, and $q_B = 4$ or 6. Methane clusters ($\rho = 0.016$ Å^{-3} per molecule) provide, according to eqs 9 and 10, the light-ion energy that is 2.56 times (for $q_B = 4$) or 3.2 times (for $q_B = 6$) larger than the light-ion energy provided by homonuclear $(D)_n$ clusters ($\rho = 0.05$ Å^{-3} per atom) with the same R_0 (see eqs 5 and 7). Next, we consider the kinematic effects. These effects modify eqs 9 and 10 when the light (A) and heavy (B) ions initially located at the same R exhibit different accelerations. The relation between the acceleration of the light (A) and the heavy (B) ions is determined by the kinematic parameter η (ref 5)

$$\eta = q_A m_B / q_B m_A \tag{11}$$

For $\eta > 1$, the light ions attain a higher acceleration than the heavy ions located initially at the same distance R. Higher acceleration leads to a higher velocity so that the light ions can overrun the heavy ions, thus attaining stronger repulsion and consequently larger kinetic energy. The reverse situation happens for $\eta < 1$. The kinematic parameters for carbon ions (B = C, $m_B = 12$) and for A = H, D, and T are presented in Table 1. The kinematic parameters for the light A atoms decrease with increasing the atom mass m_A. It follows that, in the sequence of $(CH_4)_n$, $(CD_4)_n$, and $(CT_4)_n$ clusters, the energy of the light ions is expected to decrease, while the energy of the C^{k+} ions ($k = 4$, 6) is expected to increase with increasing the mass of A^+. This isotope effect is well manifested by the simulation data in Figure 1 for the average energy (E_{av}) of H^+, D^+, T^+, C^{4+}, and C^{6+} resulting from Coulomb explosions of $(C^{4+}D_4^+)_{2171}$ produced at $I = 10^{18}$ W cm^{-2} and of $(C^{6+}D_4^+)_{2171}$ produced at $I = 10^{19}$ W cm^{-2} (A = H, D, T). Thus, E_{av} of tritons produced from the charged $(C^{k+}D_4^+)_n$ clusters is less by about 30% than E_{av} of the protons produced from the charged $(C^{k+}H_4^+)_n$ clusters for $I = 10^{18}$ W cm^{-2} (when the light ions are driven by C^{4+}), and by almost 100% for $I = 10^{19}$ W cm^{-2} (when the light ions are driven by C^{6+}) (Figure 1a). The energy E_{av} of the carbon ions produced by the charged $(C^{k+}T_4^+)_n$ clusters is larger by about 50% than that produced by the charged $(C^{k+}H_4^+)_n$ clusters (Figure 1b). The dependence of the maximum energy E_M on the kinematic parameter η is manifested in a less distinct way. The maximum energies of light ions driven by either C^{4+} or C^{6+} are almost identical for all three isotopes (Figure 1a). The difference between the isotope effects on E_{av} and E_M can be traced to the kinematic effects on the ion energy distribution (see above).

TABLE 1: Kinematic Parameters $\eta_A = q_A m_C/q_C m_A$ and $\eta_C = q_C m_A/q_A m_C$, A = H, D, and T, of the $(CA_4)_n$ Clusters

		A		
cluster	ion	B	D	T
$(C^{4+}A_4^+)_n$	A^+	3	1.5	1
	C^{4+}	0.33	0.67	1
$(C^{6+}A_4^+)_n$	A^+	2	1	0.67
	C^{6+}	0.5	1	1.5

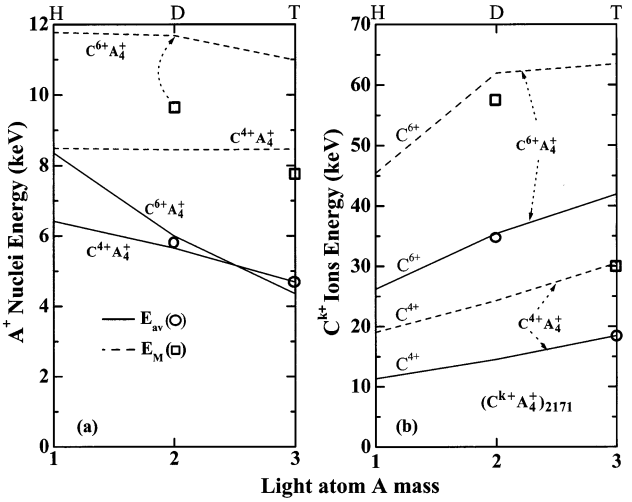

Figure 1. Dependence of the average energy E_{av} and the maximum energy E_M of ions on the mass m of the light atoms A = H, D, T for the $(CA_4)_{2171}$ clusters (radius $R_0 = 31.8$ Å). E_{av}, solid lines; E_M, broken lines. The ionized methane molecules are $C^{4+}A_4^+$ and $C^{6+}A_4^+$ at the laser intensities $I = 10^{18}$ and 10^{19} W cm^{-2}, respectively. The E_{av} (○) and E_M (□) values for vertical ionization, derived from eqs 9 and 10, are marked by circles and inserted at the m values with the kinematic parameter $\eta = 1$ ($m = 2$ for $C^{6+}A_4^+$ and $m = 3$ for $C^{4+}A_4^+$). (a) Energy of light ions A^+. (b) Energy of heavy ions C^{4+} and C^{6+}.

When the kinematic parameter is $\eta = 1$, the light and the heavy ions are expected to move with the same velocity, ensuring the validity of eqs 9 and 10. The E_{av} and E_M values of eqs 9 and 10 are marked on Figure 1 for the corresponding m_A values ($m_A = 3$ for $I = 10^{18}$ W cm^{-2} and $m_A = 2$ for $I = 10^{19}$ W cm^{-2}). The E_{av} values for $\eta = 1$ obtained from eq 10 practically coincide with the simulation results. As for the maximum energy E_M, such a coincidence occurs in one case only, namely, C^{4+}, $I = 10^{18}$ W cm^{-2} (Figure 1b). In all other cases, the E_M values of eq 9 for $\eta = 1$ are lower than the simulation values. There are two reasons for the relatively large differences between the theoretical and simulation values of E_M. First, the maximum energy E_M is much more sensitive to kinematic effects than the average energy E_{av}. Second, the direct acceleration of ions by the laser field mentioned above contributes to E_M.[6] Its contribution to E_{av} is expected to be rather small as a result of the averaging over the ions moving along the field direction and opposite to the field direction.

The energy distribution $P(E)$ of the light A^+ ions (nuclei) for the Coulomb explosion of $(C^{4+}A_4^+)_{2171}$ clusters ($I = 10^{18}$ W cm^{-2}) is shown in Figure 2a. In the case of H^+ and D^+ ions, when the kinematic parameter η is larger than unity (Table 1), the energy spectrum exhibits a large maximum located close to the maximum energy E_M. This manifestation of the kinematic effect implies that the energy of most of the product protons or deuterons lies in a relatively narrow high-energy interval. This physical situation was previously observed for D^+ ions from the Coulomb explosion of $(D_2^+O^{6+})_n$ clusters.[6] The peaked high-energy distribution for D^+ facilitates the NFDCE.[6] The energy distribution is qualitatively different for Coulomb explosion of $(C^{4+}T_4^+)_{2171}$ clusters whose kinematic parameter is $\eta = 1$. In this case, $P(E)$ increases smoothly with E up to an E value close to E_M. Such behavior is typical for homonuclear clusters under conditions of vertical ionization when the energy distribution $P(E)$ is proportional to the square root of E, according to eq 6.

The influence of the mass of the light atoms on the energy distribution of the carbon ions is demonstrated in Figure 2b for $(C^{6+}A_4^+)_{2171}$ clusters subjected to $I = 10^{19}$ W cm^{-2} irradiation. The product C^{6+} ions (carbon nuclei) for A = H and D ($\eta \leq 1$, see Table 1) exhibit a broad energy distribution, which somewhat resembles the $P(E)$ curve of the homonuclear clusters. In the case of A = T ($\eta > 1$), the energy distribution does not considerably differ from the distributions for A = H and D, except for the more pronounced maximum at the high-energy end of the energy spectrum.

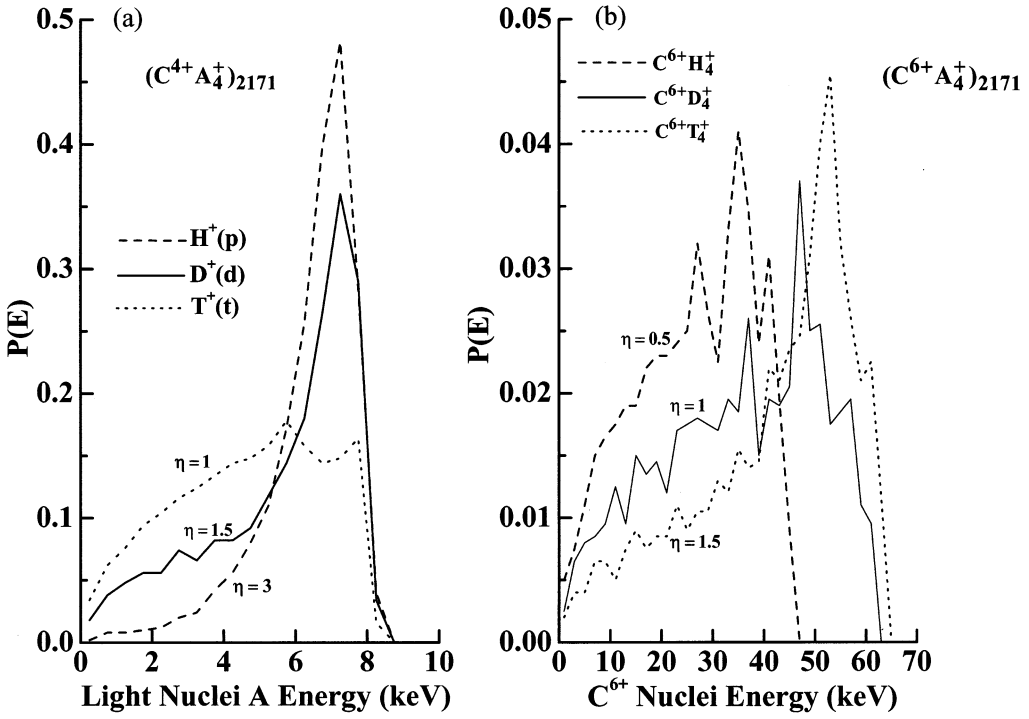

Figure 2. Kinetic energy distribution $P(E)$ of ions (nuclei) produced by Coulomb explosion of $(CA_4)_{2171}$ clusters ($R_0 = 31.8$ Å) for A = H, D, T isotopes. The $P(E)$ curves are normalized to unity. The kinematic parameters η (eq 11) are marked on the curves. (a) $P(E)$ of light A^+ ions for $I = 10^{18}$ W cm^{-2} (from $C^{4+}A_4^+$). (b) $P(E)$ of heavy C^{6+} ions for $I = 10^{19}$ W cm^{-2} (from $C^{6+}A_4^+$).

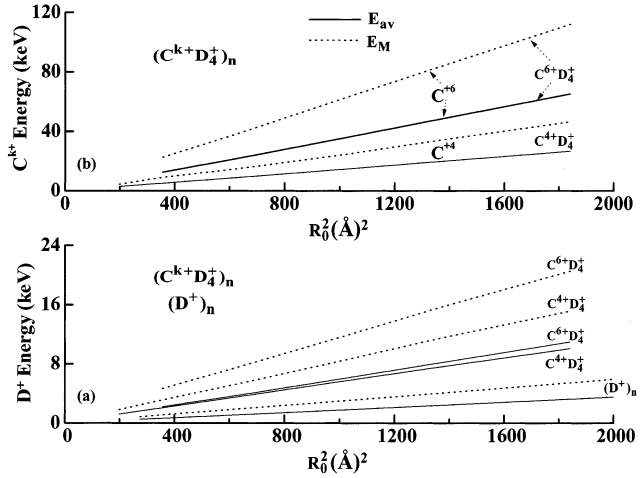

Figure 3. Dependence of the average E_{av} and maximum E_M energies of the ions on the cluster square radius R_0^2. E_{av}, solid lines; E_M, broken lines. (a) Energy of D^+ ions for Coulomb explosion of methane $(CD_4)_n$ clusters and of deuterium D_n clusters. (b) Energy of heavy ions (C^{4+} for $I = 10^{18}$ W cm^2 and C^{6+} for $I = 10^{19}$ W cm^2) for Coulomb explosion of methane $(CD_4)_n$ clusters.

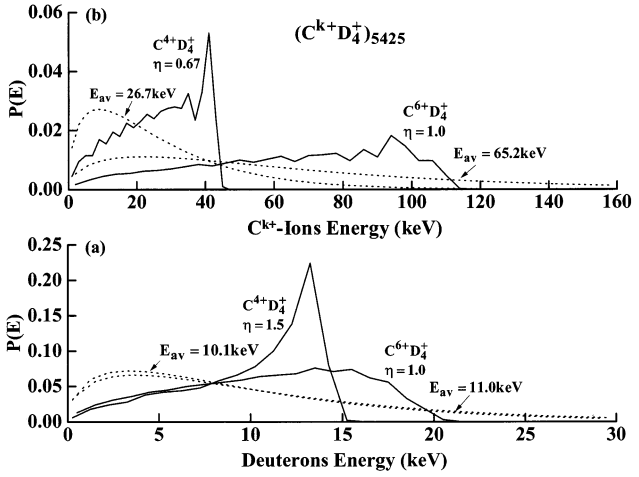

Figure 4. Kinetic energy distributions $P(E)$ of ions produced by Coulomb explosion of the $(CD_4)_{5425}$ ($R_0 = 42.9$ Å) cluster (solid lines) and of ions in thermal equilibrium (broken lines). The thermal distribution is characterized by the temperature T corresponding to the average energy E_{av} of that produced by Coulomb explosion ($^3/_2kT = E_{av}$). The $P(E)$ curves are normalized to unity. The kinematic parameters η (eq 8) and the average energies E_{av} are marked on the curves. (a) D^+ ions (deuterons d). (b) Carbon C^{4+} ions and carbon C^{6+} nuclei.

IV. Energetics of Coulomb Explosion

The ability of product deuterons to contribute to nuclear fusion is determined by their kinetic energy. As stated above, this energy increases proportionally to the square of the cluster radius, R_0^2, provided that vertical ionization conditions are satisfied. The violation of vertical ionization conditions leads first to the slowing of the energy increase[5,6] and finally to the decrease of the energy with increasing R_0.[35,36] The results of the simulations presented in Figure 3 show that, in the limit of the $(CD_4)_n$ cluster sizes considered herein ($R_0 \leq 43$ Å), the energies of the D^+, C^{4+}, and C^{6+} ions for a fixed laser intensity are well represented by the proportionality to R_0^2 (eqs 9 and 10), which indicates the validity of the vertical ionization picture. The average energies E_{av} are close to those of eq 10 for $I = 10^{19}$ W cm^{-2} when C^{6+} ions are formed and the kinematic parameter is $\eta = 1$. In the case of $I = 10^{18}$ W cm^{-2}, when C^{4+} ions are formed, eq 10 underestimates the deuteron energy ($\eta > 1$) and overestimates the carbon ion energy ($\eta < 1$) due to the kinematic effects, which were discussed in section III.

The average energy E_{av} of the deuterons (Figure 3a) is only about 9% higher for $I = 10^{19}$ W cm^{-2} (carbon ions C^{6+}) than for $I = 10^{18}$ W cm^{-2} (carbon ions C^{4+}). Taking into account the difference in the C-ion charges, the difference in the energies E_{av} (according to eq 10) is expected to be considerably larger, i.e., by 25%. The small difference between the two E_{av} values in Figure 3a can be explained by the kinematic effects in the $(C^{4+}D_4^+)_n$ cluster with $\eta > 1$, which contributes to the augmentation of the deuterons' energy. The situation is the reverse for carbon ions (Figure 3b), where the kinematic effects increase the difference between the E_{av} values of C^{4+} at $I = 10^{18}$ W cm^{-2} and of C^{6+} at 10^{19} W cm^{-2}.

The maximum size of methane clusters ($R_0 = 42.9$ Å, number of deuterons $n_D = 21\,700$) subjected herein to the $I = 10^{18}$ W cm^{-2} laser intensity provides deuterons with $E_{av} = 10.1$ keV and $E_M = 15.1$ keV. A deuterium cluster with the same size ($R_0 = 43$ Å, $n_D \approx 16530$) subjected to the same laser field provides deuterons whose energies are about three times smaller, i.e., $E_{av} = 3.43$ keV and $E_M = 5.6$ keV (Figure 3a). As expected, the energy of the carbon ions is much higher than the energy of the deuterons. For example, the maximum-size methane cluster ($R_0 = 42.9$ Å) provides C^{4+} ions ($I = 10^{18}$ W cm^{-2}) with energies $E_{av} = 25$ keV and $E_M = 65$ keV and C^{6+} nuclei ($I = 10^{19}$ W cm^{-2}) with energies as large as $E_{av} = 65.2$ keV and $E_M = 112$ keV.

The kinetic energy distribution $P(E)$ of the product ions is portrayed in Figure 4 for the maximum cluster size of $(CD_4)_{5425}$. The energy distribution of the deuterons (Figure 4a) for $I = 10^{18}$ W cm^{-2} [Coulomb explosion of $(C^{4+}D_4^+)_{5425}$] exhibits a high maximum located close to the maximum energy E_M, like in Figure 2a. As noted before, such energy distribution patterns are typical for the kinematic parameter $\eta > 1$ (Table 1). In contrast, a broad energy distribution of deuterons is exhibited for $I = 10^{19}$ W cm^{-2} [Coulomb explosion of $(C^{6+}D_4^+)_{5425}$] when the kinematic parameter is $\eta = 1$. Similar distributions characterize the C^{6+} and C^{4+} ions (Figure 4b) whose kinematic parameters are $\eta = 1$ and $\eta = 0.67$ for $I = 10^{19}$ W cm^{-2} (C^{6+}) and for 10^{18} W cm^{-2} (C^{4+}), respectively (Table 1).

The energy distributions for Coulomb explosion of methane clusters are compared in Figure 4 with the thermal distributions for the same average energies E_{av}. The energy distributions for Coulomb explosion exhibit a significantly larger fraction of high-energy particles than expected for the thermal distribution. However, the distributions obtained for Coulomb explosion lack the high-energy tail manifested for the thermal distribution (Figure 4), which is of considerable importance for thermonuclear reactions.[37]

V. Nuclear Fusion

In NFDCE experiments, the fusion reaction takes place when the energetic light nuclei (e.g., the deuterons) produced from different clusters collide with each other.[3−6] Under the conditions of the Lawrence Livermore experiment[3,4] and according to our previous analysis,[6] dd collisions occur some 70 fs after the onset of Coulomb explosion.[6] At $t > 70$ fs, the reaction volume can be described as a homogeneous gas of uniformly distributed nuclei and with randomly oriented velocities. The fusion rate in such a gas is

$$R = {}^1/_2\rho_r\langle\sigma v\rangle \qquad (12)$$

where ρ_r is the deuteron density inside the reaction volume V_r,

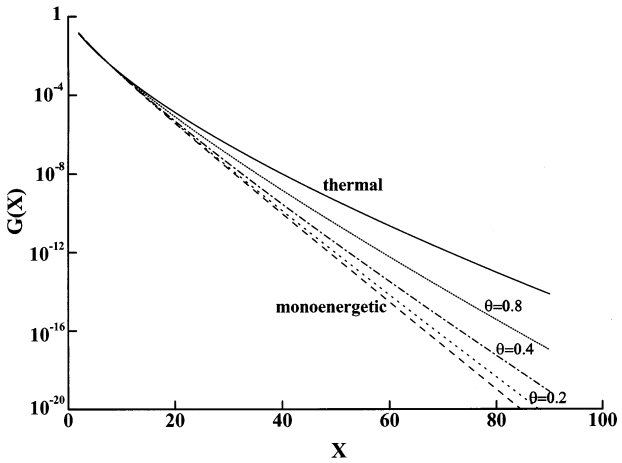

Figure 5. $G(X)$ function (eq 18) for different energy distributions. Data are given for the thermal and Gaussian energy distributions (eq 22) with different width parameters θ and monoenergetic ($\theta = 0$) energy distributions (marked on the curves).

υ is the relative velocity of the colliding nuclei, σ is the fusion cross section,[23] and the brackets mean the average over the energy distribution of the colliding nuclei.[38] Averaging over the colliding particle energies E_1 and E_2 in the laboratory frame and over the collision angle α, one obtains

$$\langle \sigma \mathrm{v} \rangle = \frac{1}{2}\int_0^\infty P(E_1)\,\mathrm{d}E_1 \int_0^\infty P(E_2)\,\mathrm{d}E_2 \int_0^\pi \sigma(E)\,(2E/m)^{1/2} \sin\alpha\,\mathrm{d}\alpha \quad (13)$$

with the energy distribution P normalized to unity. The collision energy E, which is required for the calculation of the fusion cross section, is

$$E = E_1 + E_2 - 2(E_1E_2)^{1/2}\cos\alpha \quad (14)$$

The fusion reaction cross section $\sigma(E)$ is usually expressed by the equation[23,39,40]

$$\sigma(E) = \left(\frac{S}{E}\right)\exp(-A/E^{1/2}), \quad (15)$$

where A is a constant but the parameter S depends, generally speaking, on E. Because this energy dependence is weak, in the absence of resonances, the parameter S can be considered as a constant.[19,40] The following units are used in eq 15: E in keV, S in keV cm^2, and A in keV$^{1/2}$. Substituting eq 15 with a constant value of S into eq 13 and replacing E_1 and E_2 by the dimensionless variables $x_1 = E_1/E_{\mathrm{av}}$ and $x_2 = E_2/E_{\mathrm{av}}$, one obtains

$$\langle \sigma \mathrm{v} \rangle = \xi\left(\frac{S}{A}\right)m^{-1/2}XG(X), \quad (16)$$

where m is expressed in amu and the units' transformation coefficient is $\xi = 4.395 \times 10^7$ erg$^{1/2}$ g$^{-1/2}$ keV$^{-1/2}$. X is a dimensionless parameter

$$X = \left(\frac{A}{E_{\mathrm{A}}^{1/2}}\right) \quad (17)$$

and $G(X)$ is a reduced function that is determined only by the energy distribution function

$$G(X) = \frac{1}{2}\int_0^\infty P(x_1)\,\mathrm{d}x_1 \int_0^\infty P(x_2)\,\mathrm{d}x_2 \int_0^\pi x^{-1/2} \exp(-Xx^{-1/2}) \sin\alpha\,\mathrm{d}\alpha \quad (18)$$

with

$$x = x_1 + x_2 - 2(x_1x_2)^{1/2}\cos\alpha \quad (19)$$

We note in passing that the dimensionless parameter X of eq 17 is expressed by the average energy E_{av}, whereas the corresponding parameter of ref 6 (denoted there by T_{M}) is expressed by the maximum energy E_{M}. Thus, the G functions of the present work and of ref 6 are different.

In the simplest case of monoenergetic particles (energy distribution P represented by a δ function), the G function becomes

$$G(X) = \int_0^{\pi/2} \cos\alpha \exp[-X/(2\sin\alpha)]\,\mathrm{d}\alpha \quad (20)$$

When the parameter X is large, $X \gg 1$, only α angles close to $\pi/2$ contribute to the integral of eq 20, which results in the analytical expression

$$G(X) = \frac{2}{X}\exp(-X/2)\left(1 - \frac{3}{X}\right) \quad (21)$$

Equation 21 can be used at $X > 5$ with an error of 20% for $X = 6$ and of 5% for $X = 10$. At $X > 15$, the error becomes less than 2%.

The energy distribution of the product ions of Coulomb explosion (Figures 2 and 4) is characterized by the presence of the clear-cut maximum energy E_{M} and the tendency of $P(E)$ to increase with E up to the vicinity of E_{M}. As the low-energy particles do not contribute significantly to the fusion reaction it is possible to describe the energy distribution $P(E)$ by a Gaussian, which roughly fits the high energy part of the $P(E)$ function.[6] It is convenient to represent such an energy distribution by

$$P(E) = \frac{\gamma}{\theta E_{\mathrm{av}}\sqrt{\pi}}\exp\left[-\left(\frac{E - \epsilon E_{\mathrm{av}}}{\theta E_{\mathrm{av}}}\right)^2\right], \quad (22)$$

where γ stands for the fraction of ions whose energy lies inside the Gaussian [$P(E)$ in eq 22 is normalized to γ], $E_{\mathrm{c}} = \epsilon E_{\mathrm{av}}$ is the Gaussian center, and θE_{av} is the Gaussian width. The $G(X)$ function for the arbitrary Gaussian of eq 22 is readily expressed in terms of the G function for the standard Gaussian with $\gamma = \epsilon = 1$ by the scaling relation

$$G_{\gamma,\epsilon,\theta}(X) = \gamma^2\epsilon^{-1/2}G_{1,1,\tilde{\theta}}(\tilde{X}), \quad (23)$$

where

$$\tilde{\theta} = \theta/\epsilon, \quad \tilde{X} = X\epsilon^{-1/2} \quad (24)$$

The results of the numerical integration of $G(X)$ (eq 18) for the standard Gaussian with $\gamma = \epsilon = 1$ are presented in Figure 5 for a few values of θ including the monoenergy ($\theta = 0$) case of eq 20. The $G(X)$ function for the thermal distribution is also presented in Figure 5. Using the $G(X)$ values of Figure 5 and the scaling relation in eq 23, it is possible to calculate the G function for any Gaussian energy distribution (eq 22), and consequently to determine by eq 16 the $\langle \sigma\upsilon \rangle$ value for any fusion reaction whose cross section is represented by eq 15. The dependence of $\langle \sigma\upsilon \rangle$ on the average energy E_{av} is shown in Figure 6 for the monoenergetic case, for the standard Gaussian distribution ($\gamma = \epsilon = 1$) with $\theta = 0.8$, and for the thermal distribution. Figure 6 presents $\langle \sigma\upsilon \rangle$ of the dd reaction, eq 1 ($A = 45$ keV$^{1/2}$ and $S = 1.8 \times 10^{-22}$ keV cm^2), and of the dt

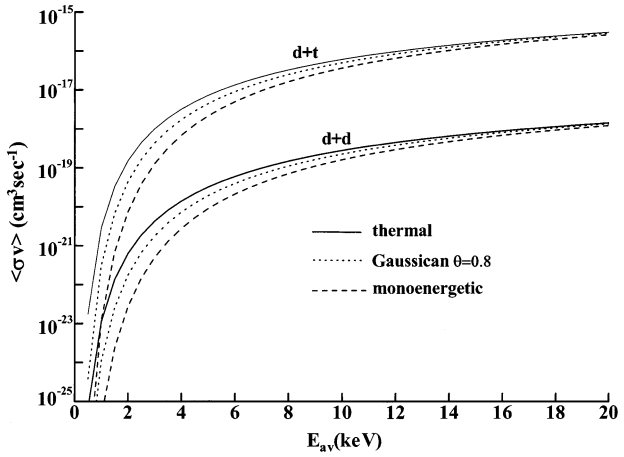

Figure 6. Dependence of the fusion parameter $\langle\sigma v\rangle$ for the dd and dt fusion reactions on the average energy E_{av} for various energy distributions. Data are given for the thermal, Gaussian (eq 22, $\theta = 0.8$), and monoenergetic ($\theta = 0$) energy distributions. The three lower curves are given for the d + d reaction (eq 1), and the three upper curves are given for the d + t reaction (eq 2).

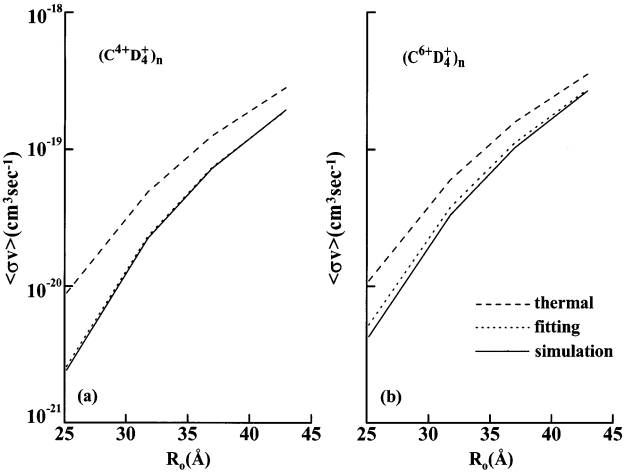

Figure 7. Dependence of the parameter $\langle\sigma v\rangle$ for the d + d fusion reaction on the cluster radius R_0 for different models of the deuteron energy distribution $P(E)$. Results are given for Coulomb explosion simulations (solid lines) and for thermal equilibrium with the same average energies E_{av} (dashed lines). We also present the $\langle\sigma v\rangle$ values obtained from a Gaussian fit of $P(E)$ (eq 22, dotted lines). (a) Ionized methane molecule $C^{4+}D_4^+$. (b) Ionized methane molecule $C^{6+}D_4^+$.

reaction, eq 2 ($A = 44$ keV$^{1/2}$ and $S = 3.4 \times 10^{-20}$ keVcm^2). The results for the dt reaction are approximate, as they were obtained by applying the expressions for identical particles to the collision of different particles. However, taking into account the closeness of the d and t masses, it is possible to expect that the errors of such an approach are not significant.

The calculation of the $\langle\sigma v\rangle$ values for the dd reaction were also performed according to eq 13 by using the energy distributions $P(E)$ from our simulations [such as $P(E)$ of Figure 5]. The dependence of these $\langle\sigma v\rangle$ values on the cluster size is presented in Figure 7, together with the $\langle\sigma v\rangle$ values of the thermal distribution for the same average energy E_{av}. For the Coulomb explosions of both $(C^{4+}D_4^+)_n$ at a laser intensity of $I = 10^{18}$ W cm^{-2} (Figure 7a) and $(C^{6+}D_4^+)_n$ at $I = 10^{19}$ W cm^{-2} (Figure 7b), the products of the Coulomb explosion of clusters exhibit a lower reaction efficiency than the thermal gas with the same E_{av} value, because of the absence of the thermal "tail". The advantage of the thermal energy distribution as compared with the energy distribution of the Coulomb-exploding clusters diminishes for large clusters with high average energy. For example, in the case of the cluster with radius $R_0 = 42.9$ Å, subjected to the laser intensity $I = 10^{19}$ W cm^{-2} ($E_{av} = 11$ keV), $\langle\sigma v\rangle = 2.7 \times 10^{-19}$ cm^2 s^{-1} (Figure 7b). A 33% higher value is produced by the thermal distribution $\langle\sigma v\rangle = 3.6 \times 10^{-19}$ cm^2 s^{-1}. In the case of a smaller cluster with $R_0 = 25.2$ Å and $E_{av} = 3.76$ keV, the thermal $\langle\sigma v\rangle$ value is 2.5 times larger than the $\langle\sigma v\rangle$ value provided by the Coulomb-exploding clusters. When the energy distribution is narrow (Figure 4a), the $\langle\sigma v\rangle$ value for the Coulomb-exploding $(C^{4+}D_4^+)_n$ cluster is well fit by the $\langle\sigma v\rangle$ value of the monoenergetic distribution with $\epsilon = 1.2$ and $\gamma = 0.8$ (Figure 7a). When the energy distribution is broad (Figure 4b), the $\langle\sigma v\rangle$ value for the Coulomb-exploding $(C^{6+}D_4^+)_n$ cluster is well fit by the $\langle\sigma v\rangle$ of the Gaussian (eq 22) for the same ϵ and γ parameters but with a finite width $\theta = 0.6$ (Figure 7b).

Using the fusion parameters obtained for the methane cluster (Figure 7) we can estimate the dd reaction yield Y per laser pulse from the relation[4,6]

$$Y = RN\,\bar{l}/\bar{v} \tag{25}$$

where R is the reaction rate (eqs 12 and 13), N is the number of deuterons in the reaction volume V_r, $\bar{l}$ is the mean path of deuterons inside the reaction volume, and $\bar{v}$ is the average velocity of the reactive deuterons. Adopting the experimental conditions of the Lawrence Livermore group,[3,4] the following parameters were used: deuteron density $\rho_r = 2 \times 10^{19}$cm^{-3}, number of deuterons $N = 1.2 \times 10^{15}$, and mean free path $\bar{l} = 0.016$ cm.[6] The velocity was identified with the maximum energy E_M.[6] In the case of the maximum cluster size used herein ($R_0 = 42.9$ Å) and laser intensity $I = 10^{19}$ W cm^{-2} ($E_{av} = 11$ keV and $E_M = 20.5$ keV), the velocity is $\bar{v} = 1.4 \times 10^8$cm s^{-1}, and the fusion parameter is $\langle\sigma v\rangle = 2.7 \times 10^{-19}$ cm^2 s^{-1} (Figure 7). Substituting these values into eqs 12 and 25, we obtain $Y = 3.7 \times 10^5$ for the neutron yield. In the experiments with deuteron clusters,[3] the yield was significantly smaller, i.e., less than 10^4. Our theoretical analysis again demonstrates the enhancement of NFDCE of heteronuclear deuterium-containing clusters. Our estimates of the nuclear fusion rates and yields consider an ensemble of heteroclusters of identical size. In the NFDCE experiments,[3,4] the ensemble of clusters corresponds to a distribution of different cluster sizes, which affects the energetics of the product nuclei and the fusion rates.[35,36] To make contact with experimental reality, our results have to be averaged over this inhomogeneous distribution of cluster sizes.

VI. Concluding Remarks

From the point of view of NFDCE, the important advantages of heteronuclear clusters involve two classes of effects: (i) energetic effects, with the heavy multielectron ions driving the light ions (nuclei), such as d or t, to considerably higher energies than for homonuclear clusters of the same size, and (ii) kinematic effects (for $\eta > 1$), which are manifested by a marked high-energy maximum in the energy spectrum near E_M that is missing in the spectrum for homonuclear clusters.[5,6] Simulations of the ionization and Coulomb explosion of the methane clusters were performed for two laser intensities, $I = 10^{18}$ and 10^{19} W cm^{-2}, that ionize the carbon atom to C^{4+} and C^{6+} (carbon nucleus) levels, respectively. In the cluster size domain considered herein, $R_0 \leq 43$ Å, the energies of both D^+ and C^{k+} ions increase proportionally to R_0^2 (Figure 3), which indicates the validity of the vertical ionization description (eqs 9 and 10). The maximum cluster size, $R_0 = 42.9$ Å, provides high-energy deuterons, i.e., $E_{av} = 11$ keV and $E_M = 20.4$ keV for $I = 10^{19}$ W cm^{-2}. Such deuterons contribute significantly to the fusion reaction, provid-

ing a fusion parameter as large as $\langle\sigma v\rangle = 2.7 \times 10^{-19}$ cm^3 s^{-1} (Figure 7) and a reaction yield of $Y \approx 4 \times 10^5$.

The efficiency of nuclear fusion depends not only on the average energy E_{av} of the colliding nuclei but also on the energy spectrum.[19,23,38] In the case of NFDCE, the energy spectrum of ions (nuclei) manifests a maximum energy onset E_M (Figures 2 and 4), in contrast to the thermal distribution with its high-energy "tail". Because of this "tail", the thermal gas provides higher (in the limits of 30−250%) fusion parameters $\langle\sigma v\rangle$. Consequently, higher fusion reaction yields are expected for the thermal gas than for the NFDCE with the same average energy of particles (Figure 7), at least in the energy domain where the reaction cross section σ increases steeply with the energy. Because of the presence of the maximum energy onset for the NFDCE, the energy spectrum of the ions produced by Coulomb explosion can be approximately described by a Gaussian function. Applying such an approach, one can determine the fusion parameter $\langle\sigma v\rangle$ by using eqs 16 and 23 and the G function of Figure 5. When the energy spectrum exhibits a sharp maximum, e.g., the case of heteronuclear clusters with a kinematic parameter $\eta > 1$ (Figures 2 and 4), it is possible to use the monoenergetic G function, which is expressed analytically by eq 21. Because of the high-energy maximum in the energy spectrum, marked enhancements of the fusion parameter and the neutron yield is then expected as a result of kinematic effects.

A search for nuclear fusion reactions involving C^{6+} that can be induced by the NFDCE is of considerable astrophysical interest.[22,23,41,42] According to our simulations, C^{6+} carbon nuclei are produced by Coulomb explosion of methane clusters $(CA_4)_n$ (A = H, D, T) at a laser intensity of $I = 10^{19}$ W cm^{-2}. The energy of the carbon nuclei is considerably higher than that of light A nuclei, for example, $E_{av} = 84$ keV and $E_M = 112$ keV in the case of the maximum cluster size $R_0 = 42.9$ Å considered herein (Figure 3b). Such an average energy corresponds to the effective temperature of $T \approx 10^9$ K, which leads, in stellar interiors, to the synthesis of heavy elements provided by $^{12}C^{6+} + {}^{12}C^{6+}$ fusion.[22,41] However, because of the limited, $E \leq E_M$, energy distribution of the $^{12}C^{6+}$ Coulomb explosion products and the short overall reaction time (~100 ps [3,4]), the detection of $^{12}C^{6+} + {}^{12}C^{6+}$ fusion in NFDCE experiments cannot be realized in real life. The minimal energy in a laboratory frame for which $^{12}C^{6+} + {}^{12}C^{6+}$ reaction cross sections are available[41] is 5 MeV, which, according to our scaling laws, can be realized for the Coulomb explosion of very large $(CD_4)_n$ clusters with radii of $R_0 \approx 300$ Å. Rough estimates performed for the reaction volume and particle density of the Lawrence Livermore experiments[3,4] result in the negligible reaction yield of $Y \approx 10^{-18}$ per laser pulse at this $^{12}C^{6+}$ energy of 5 MeV. Thus, the NFDCE of two moderately heavy nuclei, e.g., $^{12}C^{6+}$, cannot be realized. The situation looks more promising if one considers the $^{12}C(p,\gamma)^{13}N$ reaction, which is of importance in the CNO cycle in hot stars.[22,23,42] This reaction can be realized by the Coulomb explosion of $(CH_4)_n$ clusters. We used eq 15 for the $^{12}C^{6+} + {}^1H^+$ fusion reaction with the appropriate S and A parameters[42] for the estimates of the reaction yields. For the reaction volume and particle density of NFDCE experiments,[3,4] the reaction yield per laser pulse was estimated to be $Y \approx 115$ for a proton energy of $E = 150$ keV. Extrapolating the results of our simulations performed for $(CD_4)_n$ and $(CH_4)_n$ clusters for a laser intensity of $I = 10^{19}$ W cm^{-2} (Figures 1a and 3a) according to the $E_M \propto R_0^2$ scaling law, we found that the H^+ energy of ~150 keV can be provided by Coulomb explosion of $(CH_4)_n$ clusters with a radius of $R_0 \approx 120$ Å. It thus appears that some nuclear fusion reactions of heavier nuclei, e.g., $^{12}C(p,\gamma)^{13}N$, can be explored by NFDCE, providing information on the cross section and dynamics of elemental nuclear processes in astrophysics.

Acknowledgment. We are grateful to Professor John N. Bahcall for stimulating discussions on the astrophysical implications of nuclear fusion induced by Coulomb explosion of clusters. This research was supported by the James Franck Binational German−Israeli Program on Laser−Matter Interactions.

References and Notes

(1) Beuhler, R. J.; Friedlander, G.; Friedman, L. *Phys. Rev. Lett.* **1989**, *63*, 1292.
(2) Beuhler, R. J.; Friedlander, G.; Friedman, L. *Phys. Rev. Lett.* **1992**, *68*, 2108.
(3) Zweiback, J.; Smith, R. A.; Cowan, T. E.; Hays, G.; Wharton, K. B.; Yanovsky, V. P.; Ditmire, T. *Phys. Rev. Lett.* **2000**, *84*, 2634.
(4) Zweiback, J.; Cowan, T. E.; Smith, R. A.; Hurtlay, J. H.; Howell, R.; Steinke, C. A.; Hays, G.; Wharton, K. B.; Krane, J. K.; Ditmire, T. *Phys. Rev. Lett.* **2000**, *85*, 3640.
(5) Last, I.; Jortner, J. *Phys. Rev. Lett.* **2001**, *87*, 033401.
(6) Last, I.; Jortner, J. *Phys. Rev.* **2001**, *64*, 063201.
(7) Snyder, E. M.; Wei, S.; Purnell, J.; Buzza, S. A.; Castleman, A. W., Jr. *Chem. Phys. Lett.* **1996**, *248*, 1.
(8) Ditmire, T.; Tisch, J. W. G.; Springate, E.; Mason, M. B.; Hay, N.; Smith, R. A.; Marangos, J.; Hutchinson, M. H. R. *Nature* **1997**, *386*, 6, 54.
(9) Ditmire, T.; Smith, R. A.; Tisch, J. W. G.; Hutchinson, M. H. R. *Phys. Rev. Lett.* **1997**, *78*, 3121.
(10) Kondo, K.; Borisov, A. B.; Jordan, C.; McPherson, A.; Schroeder, W. A.; Boyer, K.; Rhodes, C. K. *J. Phys. B* **1997**, *30*, 2707.
(11) Lezius, M.; Dobosh, S.; Normand, D.; Schmidt, M. *Phys. Rev. Lett.* **1998**, *80*, 261.
(12) Ditmire, T.; Springate, E.; Tisch, J. W. G.; Shao, Y. L.; Mason, M. B.; Hay, N.; Marangos, J. P.; Hutchinson, M. H. R. *Phys. Rev. A* **1998**, *57*, 369.
(13) Ford, J. V.; Zhong, O.; Poth, L.; Castleman, A. W., Jr. *J. Chem. Phys.* **1999**, *110*, 6257.
(14) Köller, L.; Schumacher, M.; Köhn, J.; Tiggesbäumker, J.; Meiwes-Broer, K. H. *Phys. Rev. Lett.* **1999**, *82*, 3783.
(15) Lezius, M.; Blanchet, V.; Rayner, D. M.; Villeneuve, D. M.; Stolov, A.; Ivanov, M. Yu. *Phys. Rev. Lett.* **2001**, *86*, 51.
(16) Springate, E.; Hay, N.; Tisch, J. W. G.; Mason, M. B.; Ditmire, T.; Hutchinson, M. H. R.; Marangos, J. P. *Phys. Rev. A* **2000**, *57*, 063201.
(17) Kumarappan, V.; Krishnamurthy, M.; Mathur, D. *Phys. Rev. Lett.* **2001**, *87*, 085005.
(18) Teuber, S.; Töppner, T.; Fennel, T.; Tiggesbäumker, J.; Meiwes-Broer, K. H. *Eur. Phys. J. D* **2001**, *16*, 59.
(19) Glasstone, S.; Lovberg, R. H. *Controlled Thermonuclear Reactions*; Van Nostrand Company: New York, 1960.
(20) Krainov, V. P.; Smirnov, M. B. *JETP* **2001**, *93*, 485.
(21) Aller, L. H. *Astrophysics, Nuclear Transformations, Stellar Interiors, and Nebulae*; The Ronald Press Co.: New York, 1954.
(22) Ostlie, D. A.; Carroll, B. W. *An Introduction to Modern Stellar Astrophysics*; Addison-Wesley Co.: Reading, MA, 1996.
(23) Bethe, H. A. *Phys. Rev.* **1939**, *55*, 434.
(24) Krainov, V. P.; Smirnov, M. B. *Usp. Phys. Nauk* **2000**, *170*, 969.
(25) Ditmire, T. *Phys. Rev. A* **1998**, *57*, R4094.
(26) Last, I.; Jortner, J. *Phys. Rev. A* **2000**, *62*, 013201.
(27) Ishikava, I.; Blenski, T. *Phys. Rev. A* **2000**, *62*, 063204.
(28) Last, I.; Jortner, J. *Phys. Rev. A* **1999**, *60*, 2215.
(29) *Kirk-Othmer Encyclopedia of Chemical Technology*, 3rd ed.; John Wiley & Sons: New York, 1980; Vol. 12.
(30) Augst, S.; Meyerhofer, D. D.; Strickland, D.; Chin, S. L. *J. Opt. Soc. Am. B* **1991**, *8*, 858.
(31) Cowan, R. D. *The Theory of Atomic Structure and Spectra*; University of California Press: Berkeley, CA, 1981.
(32) Rose-Petruck, C.; Schafer, K. J.; Wilson, K. R.; Barty, C. P. J. *Phys. Rev. A* **1997**, *55*, 1182.
(33) Last, I.; Schek, I.; Jortner, J. *J. Chem. Phys.* **1997**, *107*, 6685.
(34) Heyde, P. *Basic Ideas and Concepts in Nuclear Physics*; Institute of Physics Publishing: Bristol, U.K., 1994.
(35) Parks, P. B.; Cowan, T. E.; Stephens, R. B.; Campbell, A. M. *Phys. Rev.* **2001**, *63*, 063203.
(36) Mendham, K. J.; Hay, N.; Mason, M. B.; Tisch, J. W. G.; Marangos, J. P. *Phys. Rev.* **2001**, *64*, 055201.
(37) Artsimovich, L. A. *Controlled Thermonuclear Reactions*; Gordon and Breach Science Publishers: New York, 1964.

(38) Echenique, P. M.; Manson, J. R.; Ritchi, R. H. *Phys. Rev. Lett.* **1990**, *64*, 1413.
(39) Gamov, G.; Teller, E. *Phys. Rev.* **1938**, *53*, 608.
(40) Adelberger, E. G. Austin, S.; Bahcall, J.; Balantekin, A.; Bogaert, G.; Brown, L.; Buchmann, L.; Cecil, F.; Champagne, A.; de Braeckeleer, L.; Duba, C.; Elliott, S.; Freedman, S.; Gai, M.; Goldring, G.; Gould, C.; Gruzinov, A.; Haxton, W.; Heeger, K.; Henley, E.; Johnson, C.; Kamionkowski, M.; Kavanagh, R.; Koonin, S.; Kubodera, K.: Langanke, K.; Motobayashi, T.; Pandharipande, V.; Parker, P.; Robertson, R.; Rolfs, C.; Sawyer, R.; Shaviv, N.; Shoppa, T.; Snover, K.; Swanson, E.; Tribble, R.; Turck-Chieze, S.; Wilkerson, J. *Rev. Mod. Phys.* **1998**, *70*, 1265.
(41) Barnes, C. A. In *Essays in Nuclear Astrophysics*; Barnes, C. A., Clayton, D. D., Schramm, D. N., Eds.; Cambridge University Press: Cambridge, U.K., 1982; p 193.
(42) Clayton, D. D. *Principles of Stellar Evolution and Nuclearsynthesis*; McGraw-Hill Book Company: New York, 1968.